Journal of Nonlinear and Convex Analysis
Volume 26, Number 6, 2025, 1665–1677

Yokohama Publishers
ISSN 1880-5221 ONLINE JOURNAL

WIND-INDUCED RESPONSE ANALYSIS OF THE UNDER-CONSTRUCTION TOWER-POLE COUPLING SYSTEM EXPOSED TO DOWNBURSTS

XIAOFAN LIU*, ZHIWEI LIU, AND JIAO ZHU

Abstract. The eastern coastal area of Jiangsu Province is a high occurrence area of strong convective weather, in which the downburst is a typical disaster of severe convective weather, and its sudden, localized and highly destructive nature poses a serious threat to the transmission tower line system. In this paper, taking one under-construction J1 transmission tower as an example, the wind-induce responses of the tower-pole coupling system suffering from downburst was simulated using ABAQUS software. The results show that wind-induced responses of the tower-pole coupling system are most significant during the time period of 145s to 165s. The fluctuation displacement appeared at the middle of the pole is obviously larger than those occurred at two ends. The tensioned cable experiences cyclic variations in stress, leading to potential failure of its ground anchor. For the pole body with a height of 21m in this study, two waist rings presented in Case II could exhibit an excellent displacement control, which can extremely meet the limitation required by the standard. Above findings could provide some references for the response assessment of the tower-pole coupling system under downbursts.

1. Introduction

Transmission towers are characterized by their properties of lightweight, highly flexibility and small damping, belonging to a kind of wind sensitive structures. The strong convective weathers, such as thunderstorms, tornadoes and downbursts, become the main environmental factors causing structural damage and even collapse of these transmission towers [1,13,15,22]. Over the past 50 years, meteorological observations in China have shown that the severe convective weathers occur frequently in the season of summer and that the downbursts associated with thunderstorms become the major events appeared in the strong winds [5,10,17,25]. A downburst is a short-term destructive high intensity wind generated in the near ground area by a strong sinking airflow generated by thunderstorm weather [9], which violently impacts the ground. It has the characteristics of suddenness, locality, short period, and high outflow intensity [5,7]. In recent decades, the safety of transmission tower-line system under the action of downburst has received widespread attention all over the world, and numerical simulation methods have been popularly utilized

2020 *Mathematics Subject Classification.* 90C35, 93C41, 68U35, 62H25.

Key words and phrases. Downburst, under-construction transmission tower, tower-pole coupling system, wind-induced response, reinforcement measure .

This research is financially supported by State Grid Jiangsu Electric Power Co., Ltd., China (No. J2023090).

*Corresponding author.

to investigate the downburst wind loads, wind-induced vibration response, and instability collapse of the system [14, 19].

In terms of the downburst wind loads acting on the transmission tower-line system, an OBV model, which represented the wind speed profile model, was proposed and improved by Oseguera and Bowles [16], and Vicroy [20]. Damatty and Elawady [10] proposed three typical scenarios under downburst conditions and explored the load distributions on six different types of transmission towers. Zhang and Xie [23] conducted a failure analysis of a damaged transmission line caused by a typhoon and exhibited a limit load investigation on the transmission tower. For the issues on the vibration of tower-line system induced by downbursts, Fang et al. [8] carried out a nonlinear dynamic analysis of a single transmission tower and a tower-line system to reveal their vibration responses induced by downburst wind and pointed out that the resonance response of the tower-line system decreased due to the existence of the lines. Ahmed and Damatty[3] studied the wind-induced vibration response of a tower-line system under downburst and the outcomes derived from numerical simulations indicated that the speed of downburst movement had a relatively small impact on the wind-induced vibration response of the system. In addition, several research works have been conducted on the instability and even collapse of the tower-line system suffering from the action of downbursts. The findings proposed by Zhang and Xie [23] indicated that the buckling of the diagonal bracing under the influence of the typhoon was the main cause of instability of the transmission tower. Tian et al. [18] completed a full-scale experimental investigation on a steel pipe truss transmission tower and concluded that the buckling failure of the tower leg components was the main cause of the tower collapse. Zheng and Fan [24] simulated the progressive collapse patterns of a transmission tower-line system under downburst loading and verified that the movement path of downburst center significantly affected the collapse of the system. These above studies can provide valuable references for understanding the stress characteristics, vibration responses, and collapse mechanisms of the transmission tower-line system under downbursts. However, a unified design method for wind resistance of transmission towers against downbursts has not yet been established, and there is a lack of research on the wind-induced vibration response and failure mechanism of the incomplete under-construction transmission tower. Therefore, further attentions are needed to be paid on these areas.

In view of this, the present study focuses on the wind-induced vibration of an under-construction tower in the Yilu-Xuwei 500 kV transmission line (abbreviated as 'Yixu Line') in Jiangsu Province, China. In response to the strong wind environment caused by downburst, the wind-induced vibration response of the tower-pole coupling system in an under-construction tower (see Figure 1) was analyzed using a dynamic finite element analysis method. By applying quasi-static equivalent wind loads, the weak positions of this tower-pole coupling system were identified under the condition of downburst. Accordingly, the whole safety of the under-construction tower was assessed during different construction phases. The work presented here

can provide some useful references for the safety evaluation of under-construction transmission towers subjected to downbursts.

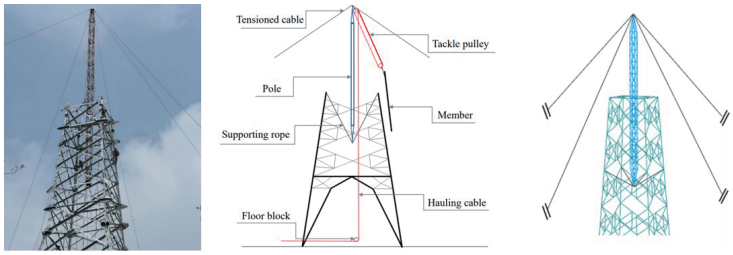

FIGURE 1. Transmission tower-pole coupling system under construction.

2. Establishment of FE model for tower-pole coupling system

The 'Yixu Line' mainly adopts four types of transmission tower, 500-KM21D-J1 (hereinafter referred to as J1), 500-KM21D-J3, 500-KM21D-Z1 and 500-KM21D-Z2, and all of them utilize the construction method of tower-pole coupling system. Here, the J1 tower is primarily discussed in this study. The tower body is mainly made of angle steel elements, with strength grades of Q235, Q345, and Q420. The main element in the pole is the steel pipe with a strength grade of Q345. The pole is composed of a 28m long steel pipe grid structure with a diameter of 550mm, in which the chord members are steel pipes with a diameter of 32 mm and a thickness of 2.5mm, and the diagonal and horizontal bars are steel pipes with a diameter of 50 mm and a thickness of 3mm. The internal supporting ropes and external tensioned cables of the pole are made of 22 mm and 16 mm steel strands, respectively.

Using the ABAQUS finite element (FE) software, numerical calculations are conducted on the wind resistance performance of the tower-pole coupling system during construction. In the FE model indicated in Fig.1(c), both the angle steel in the tower body and the steel pipe used in the pole are modeled using T3D2 truss elements. The constitutive model for them is an ideal elastic-plastic model with an elastic modulus of $2.1 \times 105MPa$ and a Poisson's ratio of 0.3. To simulate the tensioned state in the cables and supporting ropes, a 'cooling method' is used to induce pre-stressing force in the cables and ropes, which can simulate the tensioned state of steel strands. The tower foot is rigidly connected, and both ends of tensioned cables are hinged. PIN coupling connection is configured at two ends of the supporting rope, which allows for free rotation at the hinge point. The nonlinear implicit dynamic method is utilized in the calculation, which can accurately simulate the dynamic characteristics of the established model.

3. Wind field simulation of downburst

The boundary layer wind of strong convective weather is usually composed of a mean wind with a duration exceeding 10 minutes and a fluctuating wind with

a duration of only a few seconds to tens of seconds [6]. Among them, the period of mean wind is generally much greater than the natural vibration period of the tower structure. Therefore, the action caused by mean wind can be simplified as a static behavior. While, the intensity of fluctuating wind exhibits great randomness over time, which can easily cause significant dynamic responses in tower structures. Therefore, according to the above definition of the boundary layer wind, the wind speed of downburst at different heights could consist of a mean wind speed and a fluctuating wind speed [6], as given in Eq.(3.1).

$$U(z,t) = \bar{U}(z,t) + u(z,t) \tag{3.1}$$

where, $U(z,t)$ is the instantaneous wind speed of downburst at any height z and time t; $\bar{U}(z,t)$ and $U(z,t)$ are the corresponding mean wind speed and fluctuating wind speed, respectively.

3.1. **Mean wind speed of downburst.** Chen and Letchford [20] proposed a mixed stochastic model that considered the pulsation characteristics of downburst, in which the average wind speeds at different heights were assumed to simultaneously reach their maximum values. In accordance with this assumption, the mean wind speed of downburst can be determined by the product of a space function of wind speed and a time function, as:

$$\bar{U}(z,t) = V(z,t)\, d(t) \tag{3.2}$$

where, $V(z)$ is the space function of the maximum mean wind speed and d(t) is a time function with a maximum value of 1. In terms of the space function $V(z)$, some researchers, such as Oseguera and Bowles [16] and Vicroy [20] (OBV model), Wood et al. [21] (Wood model), Holmes and Oliver [11] (Holmes model) have proposed their respective model to evaluate the mean wind speed profile of downburst through experimental investigations and numerical simulations. In this study, the Vicroy model [20] is utilized for calculation as its simulation results usually show a better fitting effect. Accordingly, the vertical profile of the maximum mean wind speed in downburst V(z) can be described as Eq.(3.3). Figure 2(a) depicts the typical variation curves of $V(z)$ as the vertical height increases up to 400m.

$$V(z) = 1.22 * \left[e^{(-0.15z/z_{max})} - e^{(-3.2175z/z_{max})}\right] * V_{max} \tag{3.3}$$

where, z is the vertical height; V_{max} is the maximum horizontal wind speed on the vertical wind profile of the downburst; z_{max} is the height corresponding to V_{max}.

The time function d(t) can describe the time-varying characteristic of mean wind speed at a specific location during the development of a downburst, which can be expressed with Eq.(3.4) using the wind speed vector $V_c(t)$.

$$d(t) = \frac{|V_c(t)|}{max|V_c(t)|}. \tag{3.4}$$

Holmes and Oliver [11] proposed that the wind speed vector $V_c(t)$ at any observation point in the downburst wind field could be obtained by vector addition of the radial wind speed $V_r(t)$and the downburst center moving speed $V_{(t)}$, that is $V_c(t) = V_r(t) + V_t$. Due to the fact that the mean wind speed of downburst is much greater than its moving speed, the change in the direction of mean wind speed caused by

the movement of downburst can be usually ignored [2,3,8]. Accordingly, the impact of downburst movement on $V_c(t)$ could not be considered here. Then the size of vector$V_r(t)$ could be expressed by Eq.(3.5) and [11]. Figure 2(b) shows the typical variation curves of $V_r(t)$ as the radial distance increases up to 3000m.

$$V_r(t) = V_{r,max}(r/r_{max}).....0 \leqslant r < r_{max} \tag{3.5}$$
$$V_{r,max}e^{(-[r-r_{max}/R_r]^2)}.....r \geq r_{max}$$

where, $V_{r,max}$ is the maximum value of the radial wind speed profile; r_{max} is the radius from the wind center to the location of $V_{r,max}$; r is a radial distance; R_r is a radial length scale and its usual value is $1/2r_{max}$.

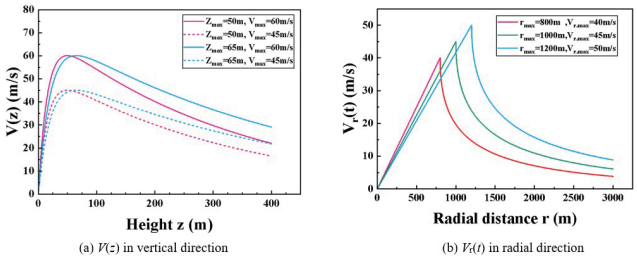

(a) $V(z)$ in vertical direction (b) $V_r(t)$ in radial direction

FIGURE 2. Mean wind speed profiles of downburst.

3.2. **Fluctuating wind speed of downburst.** The downburst fluctuating wind speed has obvious non-stationary characteristics, which can be expressed by utilizing a modulation function [6]. Then, the fluctuating wind speed u(z, t) can be described by a product of a time-dependent modulation function a(z, t) and a stationary Gaussian random process k(z, t)[16, 20], given as:

$$u(z,t) = a(z,t).k(z,t). \tag{3.6}$$

In Eq.(3.6), the modulation function $a(z,t)$ can be approximately expressed with $(0.08-0.11)$. The Gaussian random process $k(z,t)$ with zero mean and variance of 1 can be expressed by Eq.(3.7) with a given spectrum.

$$k(z,t) = \int_{-x}^{+x} e^{i\omega x} dZ(Z,\omega). \tag{3.7}$$

where, $Z(z,\omega)$ is an orthogonal increment process with height z and natural frequency ω and it can be described by Eq.(3.8); in which, $E(.)$ is the mathematical expectation and $\phi(z,\omega)$ is a power spectral density function, which can be normalized into a scalar using Eq.(3.9).

$$E\left\{|dZ(z,\omega)|^2\right\} = \phi(z,\omega)d\omega, \tag{3.8}$$

$$\int_{-x}^{+x} \phi(z,\omega)d\omega = 1. \tag{3.9}$$

Here, the Kaimal spectrum [24] was adopted to calculate $\phi(z,\omega)$, making it obey the standard normal distribution. The corresponding process can be calculated by Eq.(3.10).

$$\phi(z,\omega) = \frac{1}{2}\frac{200}{2\pi}u_*^2\frac{z}{V_t}\frac{1}{[1+50\frac{\omega z}{2\pi V_t}]^{5/3}\frac{1}{6u_*^2}} \tag{3.10}$$

where, u_* is the radial shear velocity of wind; ω is in the range of $[-\pi,\pi]$.

3.3. **Wind field simulation of downburst.** For a typical downburst, assuming that $z_{max} = 65m$, $V_{max} = 60m/s$ (see Figure 2(a)), and $r_{max} = 1000m$, $V_{r,max} = 45m/s$ (see Figure 2(b)), and $u* = 1.76m/s$ [6], $V_t = 8m/s$, the wind speed-time histories at any height can be calculated using Eqs. (3.1)–(3.10) and the outcomes at heights of $10m$ and $38m$ are displayed in Figure 3.

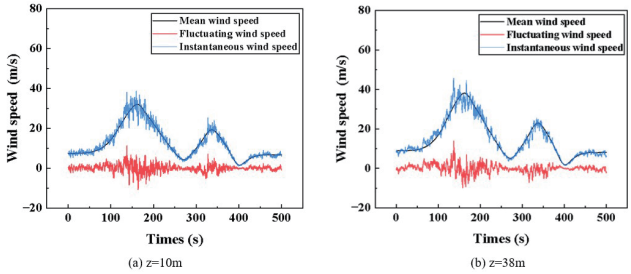

FIGURE 3. Simulated wind speed-time history curve of downburst.

3.4. **Determination of wind loads of downburst.** For one under-construction transmission tower, the peak reaction induced by wind loads is typically achieved when the tower is located at the center of downburst. Consequently, the loading sections of wind loads in the tower-pole coupling system can be displayed in Figure 4(a). In accordance with the guidelines for electrical transmission line structural loading [4], the downburst wind load acting on each loading section can be determined with Eq. (3.11).

$$\begin{aligned} F_x &= 0.5\rho U(z,t)^2\cos^2\alpha C_x S_x, \\ F_y &= 0.5\rho U(z,t)^2\sin^2\alpha C_y S_y \end{aligned} \tag{3.11}$$

where, ρ is the density of air with $\rho = 1.29kg/m^3$; α is the wind direction angle corresponding to x direction; C_x and C_y are the resistance coefficients in x and y directions, respectively; S_x and S_y are the effective windshield areas in x and y directions of the transmission tower.

As indicated by the ABAQUS model in Figure 4(a), the wind loading points are arranged every 5 meters on the main elements of the tower-pole coupling system. The uniformly distributed load of the simulated downburst wind is simplified as a concentrated force acting at the loading point in the y-direction. Finally, for the J1 under-construction tower with a working height of 35m determined at the pole's

bottom, as shown in Figure 4(a), there are 14 loading points placed on the tower and 6 loading points acted on the pole. Besides, for an under-construction transmission tower under downbursts, numerical calculation using ABAQUS can take account of the geometric nonlinearity, and the explicit dynamics algorithm method can be utilized for the transient dynamic analysis.

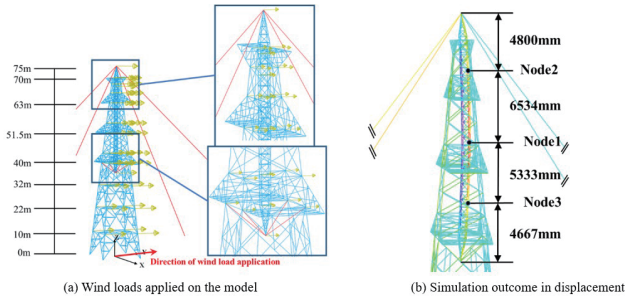

(a) Wind loads applied on the model (b) Simulation outcome in displacement

FIGURE 4. ABAQUS model of the tower-pole coupling system of J1 tower under downburst.

4. Results and discussions

By using the above established ABAQUS model and wind field in Figure 3 ($V_{max} = 60m/s$), the displacement developments and stress changes of the tower-pole coupling system under different construction conditions can be obtained within the period of calculation time, as shown in Figuref 4(b). A comparison among the calculation results indicate that the wind-induced response of the tower-pole coupling system are most significant during the time period of $145s$ to $165s$, which is consistent with the time interval during which the maximum wind speed of downburst is reached (see Figure 3). Therefore, the following results and discussions will focus on the outcomes simulated within this time interval.

4.1. **Displacement responses at two ends of the pole.** Figure 5 indicates the displacement variations at the top end (hinged to the tensioned cable) and bottom end (hinged to the supporting rope) of the pole. It can be observed from Figure 5 that under a maximum wind speed of $60m/s$, the displacements measured at the top and bottom ends of the pole present varying degrees of fluctuations. At bottom end of the pole, the displacement varies within a small range of $-0.5mm \sim 2.5mm$. While, a large displacement fluctuation still occurs at top end of the pole, despite it is constrained by four tensioned cables. The maximum displacement in the y-direction can reach $31.6mm$. By comparison, it can be concluded that the wind-induced displacement response at the top of the pole is relatively significant, which should become a position that needs to be carefully monitored and controlled.

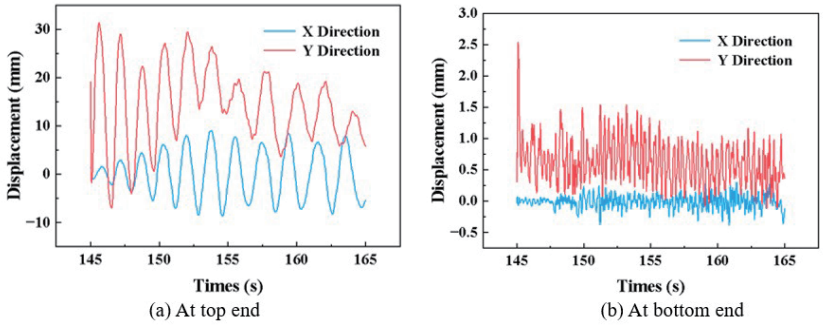

FIGURE 5. Displacement response at top and bottom ends of the pole under downburst.

4.2. **Stress responses in tensioned cables and supporting ropes.** The stress changes in the tensioned cable and supporting rope are depicted in Figure 6(a) and (b), respectively. Similar to the displacement response in Figure 5, Figure 6 also exhibits a fluctuation process of the stresses in tensioned cables and supporting rope. Specifically, the tensioned cable experiences cyclic variations in stress, as shown by the oscillatory pattern in Figure 6(a). This behavior is primarily driven by the dynamic wind loads characteristic of downbursts, which subject the cable to alternating compressive and tensile forces. In contrast, the supporting rope, depicted in Figure 6(b), shows a more irregular force distribution. The variations are less periodic and suggest a complex interaction between the dynamic loading conditions and the inherent flexibility of the rope.

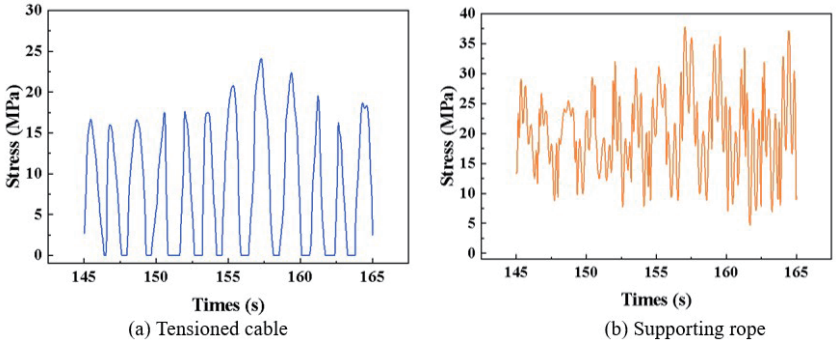

FIGURE 6. Stress responses in the tensioned cable and supporting rope under downburst.

Although the downburst-induced stresses in the tensioned cable and supporting rope exhibit distinct temporal and magnitude characteristics, it can be believed that these stresses in the cable and rope are safe for the steel strands adopted in J1 tower. In addition, due to the cyclic stress variations in the tensioned cable, it should pay more attentions to the safety of its ground anchor during downburst.

4.3. **Wind-induced responses of the tower-pole system under various conditions.** When the wind speed $_{V}max$ in downburst increase from $40m/s$ to $60m/s$, the variations in the displacement and stress responses in the tower-pole coupling system at working height of 35m are displayed in Table 1, which provides a comprehensive overview of the maximum stresses experienced by the tower elements, tensioned cables, and supporting ropes, as well as the maximum displacement appeared in the pole under varying wind speeds of downburst. Increasing V_{max} from $40m/s$ to $60m/s$, a clear trend of rising the displacement of the pole is evident, reflecting the increasing structural demands imposed by higher wind loads. For instance, at a wind speed of $60m/s$, the maximum displacement in the pole reaches $826.4mm$, while the tensioned cable and supporting rope experience stresses of $12.06MPa$ and $13.75MPa$, respectively. This indicates the displacement occurred at the near middle of pole plays a critical role in maintaining stability and safety under extreme wind conditions.

TABLE 1. Comparison of displacement and stress in J1 tower under different V_{max}.

Table 1 Comparison of displacement and stress in J1 tower under different V_{max}				
V_{max} (m/s)	Maximum displacement in the pole (mm)	Maximum stress (MPa)		
		Tower	Tensioned cable	Supporting pole
40	659.2	31.9	9.63	12.54
45	688.6	33	9.82	12.76
50	720.3	34.4	10.98	13.08
55	766.8	35.2	11.23	13.45
60	826.4	37.6	12.06	13.75

During the construction period of transmission tower, the pole will be raised gradually to meet the construction requirements. Table 2 compares the wind-induced responses of the pole at different working heights of $30 \sim 45m$ (determined at bottom of pole) when V_{max} is $60m/s$. As indicated in Table 2, the stress and displacement of the pole increase gradually with increasing its working height, especially the displacement measured near the middle of height.

These above results present the significant wind-induced displacement response of the pole under the different wind speed and construction phase and emphasize the need for careful design considerations to mitigate the potential risks posed by downbursts. Besides, except the huge displacement, the swing phenomenon of the pole is also evident during the action of downburst. A typical swing process of the pole in a short period of $153s$ to $155s$ at$_{Vmax}$ $= 60m/s$ is depicted in Figure 7. Therefore, controlling the displacement response of the pole induced by downburst seems to be important to ensure the safety of tower-pole coupling system during construction.

TABLE 2. Comparison of displacement and stress in pole at different working height.

Table 2 Comparison of displacement and stress in pole at different working height				
Working height (m)	Maximum stress (MPa)	Displacement (mm)		
		Near middle	At top	At bottom
45	50.3	876.7	36.1	4.7
40	46.6	828.3	33.8	4.1
35	42.4	792.3	30.2	3.6
30	38.9	743.5	27.6	3.4

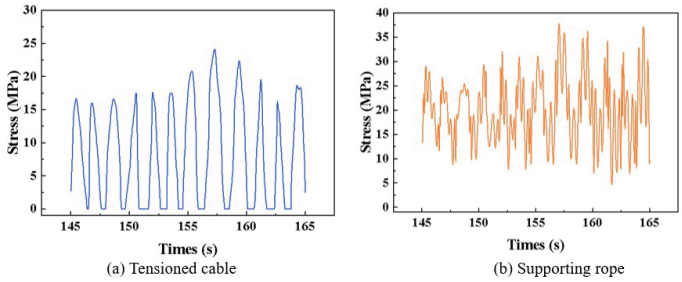

(a) Tensioned cable (b) Supporting rope

FIGURE 7. Swing characteristic of the pole during a short period.

4.4. **Displacement response control of the pole with reinforcement measures.** In terms of the pole, the largest downburst-induced displacement usually occurs at its middle zone, which can reach to $826.4mm$ under wind speed of $60m/s$, as shown in Figure 8. According to the Chinese standard of GB $50135-2019$ [9], the horizontal displacement at any point of a tall structure should not exceed $1/100$ of its height from the ground. In this study, the total height of the pole is 21 meters and its one percent is $210mm$. It is evident that the horizontal displacement of the pole significantly exceeds the limitation specified by the above standard. If the wind speed continues to rise, the stability of the tower-pole coupling system may be jeopardized, potentially leading to the failure of whole structure. In order to mitigate the swing amplitude of the pole under downburst and minimize the risk of collision with other elements in the under-construction tower, the waist ring is commonly utilized as one kind of reinforcement measures to control the displacement of the pole.

In this study, the reinforcement effect of configuring waist rings on the pole's displacement will be assessed by considering three following cases: 1) Case I: one waist ring set at $1/2$ height of the pole; 2) Case II: two waist rings placed at nearly $1/5$ and $2/3$ height, and 3) Case III: three waist rings fixed at nearly $1/5$, $2/4$ and $2/3$ height. It should be noted that the selection of these positions for installing the waist rings depends on the location of the cross-beam in tower. Besides, in the ABAQUS FE model, the waist rings are modeled using TRUSS elements, with material properties consistent with those of the rope. After simulations under the

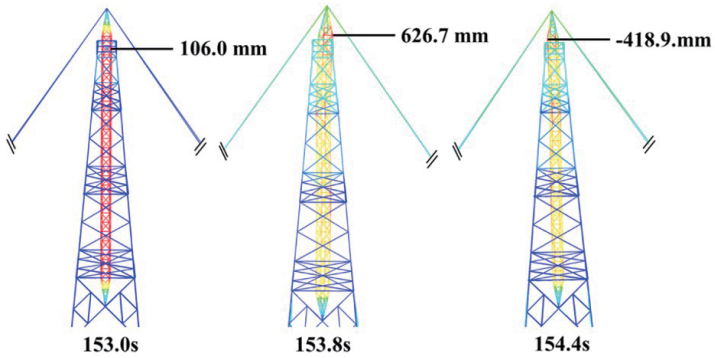

FIGURE 8. Maximum displacement of the rope (Zoom in 100 times)

same downburst with wind speed of $60m/s$, the displacements of the pole with various waist rings are illustrated in Figure 8.

It can be observed from Figure 8 that the maximum horizontal displacement of the pole decreases significantly with the increase in the number of waist rings from Case I to Case III. Taking three observation nodes shown in Figure 4 into account, the impact of waist rings on diminishing the displacement of the pole is compared and the corresponding outcome is plotted in Figure 9. The findings indicated in Figure 9 demonstrate that the addition of waist rings is a useful way to control the horizontal displacement of the pole under downburst. For a pole with a height of $21m$ in this study, both Case II and Case III reinforcement schemes demonstrate excellent displacement control of the pole. According to the construction convenience and economy, the two waist rings presented in Case II can meet the limitations of the standard requirements extremely well. According to the research results, this paper proposes the most economical and effective reinforcement suggestions for the poles of long steel pipe grid structure. When the poles encounter downburst, a waist ring is installed every $7 \sim 8m$ in the middle of the poles to control the lateral displacement.

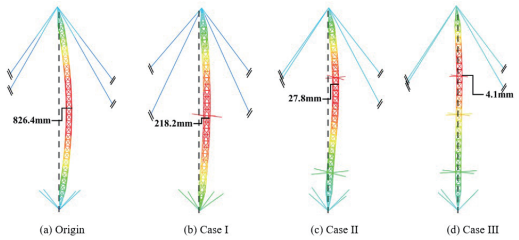

FIGURE 9. Variations of maximum displacement in the pole with waist rings.

5. Conclusions

This study presents a comprehensive analysis of the wind-induced responses of a tower-pole coupling system under downbursts. The following conclusions can be drawn:

1) An ABAQUS FE model is proposed to simulate the vibration response of an under-construction tower-pole coupling system under the action of downburst. In the model, the wind field of downburst consists of a mean wind and a fluctuating wind and the corresponding wind loads are simplified as concentrated forces acting on the system.

2) For the tower-pole coupling system under downburst, the displacement fluctuation response at the top of the pole is significant and accordingly its tensioned cables experience cyclic variations in stress, which will induce potential failure of their ground anchors during downburst.

3) Due to the high flexibility of pole body, a large downburst-induced displacement would occur at its near half of the height, which greatly exceeds the limitation of horizontal displacement. The addition of waist rings around the pole can effectively reduce its displacement. It is recommended to install a waist ring at every $7 \sim 8$ meters along the pole, which can provide valuable guidance for controlling the pole's displacement during a downburst.

References

[1] E. S. Abd-Elaal, J. E. Millsa and X. Ma, *A review of transmission line systems under downburst wind loads*, Journal of Wind Engineering and Industrial Aerodynamics **179** (2018), 503–513.

[2] H. Aboshosha and A. El Damatty, *Dynamic response of transmission line conductors under downburst and synoptic winds*, Wind and Structures **21** (2015), 241– 272.

[3] A. Ahmed and A. El Damatty, *Dynamic response of conductors during transmission tower failure under downburst loads*, Engineering Structures **305** (2024): 117727.

[4] American Society of Civil Engineers (ASCE), *Guidelines for Electrical Transmission Line Structural Loading (fourth ed.)*, USA: ASCE Manuals and Reports on Engineering Practice, (2020). `https://ascelibrary.org/doi/pdf/10.1061/9780784415566.fm`

[5] M. T. Chay, F. Albermani and R. Wilson, *Numerical and analytical simulation of downburst wind loads*, Engineering Structures **28** (2006), 240–254.

[6] L. Chen and C. W. Letchford, *A deterministic-stochastic hybrid model of downbursts and its impact on a cantilevered structure*, Engineering Structures **26** (2004), 619–629.

[7] A. El Damatty and A. Elawady, *Critical load cases for lattice transmission line structures subjected to downbursts: economic implications for design of transmission lines*, Engineering Structures **159** (2018), 213–226.

[8] Z. Fang, Z. Wang, R. Zhu and H. Huang, *Study on wind-induced response of transmission tower-line system under downburst wind buildings* **12** (2022): 891.

[9] GB 50135-2019, *Standard for Design of High-rising Structures*, Ministry of Housing and Urban-Rural Development of the People's Republic of China, (2019). `https://www.scribd.com/document/686658679/GB-50135-2019-Standard-for-Design-of-High-rising-Structures`

[10] M. Hadavi and D. Romanic, *Atmospheric conditions conducive to thunderstorms with downbursts in Canada and a downburst precursor parameter*, Atmospheric Research **305** (2024): 107428.

[11] J. D. Holmes and S. E. Oliver, *An empirical model of a downburst*, Engineering Structures **22** (2000), 1167–1172.
[12] J. C. Kaimal, J. C. J. Wyngaard, Y. Izumi and O. R.Coté, *Spectral characteristics of surface-layer turbulence*, Quarterly Journal of the Royal Meteorological Society **98** (1972), 563–589.
[13] H. Li, B. Li, J. Yao, S. Hu and F. Yang, *Refined simulation of strong convective winds in Jiangsu and its application to tower level disaster prevention and forecast of power grid*, Procedia Computer Science **224** (2023), 395–400.
[14] L. Li, *Measures to improve the wind resistance of 500 kV transmission lines in coastal typhoon areas*, Energy and environment **04** (2020), 113–116.
[15] S. Li, R. A. Catarelli, B. M. Phillips, J. A. Bridge and K. R. Gurley, *Physical simulation of downburst winds for civil structures: A review*, Journal of Wind Engineering and Industrial Aerodynamics **254** (2024): 105900.
[16] R. M. Oseguera and R. L. Bowles, *A simple, analytic 3-dimensional downburst model based on boundary layer stagnation flow*, Hampton: NASA Technical Memorandum, 1988.
[17] G. Solari, *Emerging issues and new frameworks for wind loading on structures in mixed climates*, Wind and Structures **19** (2014), 295–320.
[18] L. Tian, H. Pan, R. Ma, L. Zhang and Z. Liu, *Full-scale test and numerical failure analysis of a latticed steel tubular transmission tower*, Engineering Structures **208** (2020): 109919.
[19] B. C. Vermeire, L. G. Orf and E. Savory, *Improved modelling of downburst outflows for wind engineering applications using a cooling source approach*, Journal of Wind Engineering and Industrial Aerodynamics **99** (2011), 801–814.
[20] D. D. Vicroy, *Assessment of microburst models for downdraft estimation*, Journal of Aircraft **29** (1992), 1043–1048.
[21] G. S. Wood, K. C. Kwok, N. A. Motteram and D. F. Fletcher, *Physical and numerical modelling of thunderstorm downbursts*, Journal of Wind Engineering and Industrial Aerodynamics **89** (2001), 535–552.
[22] Q. Yang, J. Yin, M. Liu, Y. Wang, Y. Hui, S. Li and S. Hamza, *Post-disaster investigations of damage feature of buildings and structures due to several local strong winds in China during 2021–2024*, Advances in Wind Engineering **1** (2024): 100011.
[23] J. Zhang and Q. Xie, *Failure analysis of transmission tower subjected to strong wind load*, Journal of Constructional Steel Research **160** (2019), 271–279.
[24] H. D. Zheng and J. Fan, *Progressive collapse analysis of a truss transmission tower-line system subjected to downburst loading*, Journal of Constructional Steel Research **188** (2022): 107044.
[25] C. Zhu, Q. Yang, G. Huang, X. Zhang and D. Wang, *Fragility analysis and wind directionality-based failure probability evaluation of transmission tower under strong winds*, Journal of Wind Engineering and Industrial Aerodynamics **246** (2024): 105668.

Manuscript received October 8, 2024
revised December 20, 2024

X. Liu
State Grid Jiangsu Electric Power Co., Ltd. Construction Branch, Nanjing Jiangsu 210011, China
E-mail address: jackyone1981@yeah.net

Z. Liu
State Grid Jiangsu Electric Power Co., Ltd. Construction Branch, Nanjing Jiangsu 210011, China
E-mail address: 15951015099@163.com

J. Zhu
State Grid Jiangsu Electric Power Co., Ltd. Construction Branch, Nanjing Jiangsu 210011, China
E-mail address: zhujiao90@163.com